



Influence of interconnect resistances on parallel-connected LiFePO₄ cells performance

Long Chang, Bin Duan, Peng Li, Kang Zhang, Chenghui Zhang
and Linjing Xiao

EasyChair preprints are intended for rapid dissemination of research results and are integrated with the rest of EasyChair.

October 3, 2019

Influence of interconnect resistances on parallel-connected LiFePO₄ cells performance

Long Chang

School of Mechanical and Electronic Engineering
Shandong University of Science and Technology
Shandong University
Qingdao, China
lchang@sdu.edu.cn

Bin Duan

School of Control Science and Engineering
Shandong University
Jinan, China
duanbin@sdu.edu.cn

Peng Li

Biomedical Engineering Department
The Affiliated Hospital of Qingdao University
Qingdao, China
lpbelieveyou@126.com

Kang Zhang

China Academy of Machinery Science & Technology Qingdao Branch Co., LTD.
Qingdao, China
zhang_kang20@163.com

Chenghui Zhang

School of Control Science and Engineering
Shandong University
Jinan, China
zchui@sdu.edu.cn

Linjing Xiao

Shandong University of Science and Technology
Qingdao, China
xiaolj2008@126.com

Abstract—The battery module of parallel-connected lithium-ion cells is extensively applied in electric vehicles to satisfy the capacity and power capability. However, the performance of the module is influenced by the interconnect resistances and the position of its current collector. An equivalent circuit simulation model is developed and validated by pulse discharge tests. Based on the model, a module of five cells connected in parallel is established, including interconnect resistances. Then the effect of interconnect resistances and different positions of module current collector in parallel-connected cells is tested and discussed by the simulation. Results indicate that the interconnect resistances lead to inhomogeneous currents, and the cell directly connected to the module current collector appears the highest current. That is, the farther the cell is away from the module current collector, the lower current is. The cause are clarified from an angle of the currents through interconnect resistances. Therefore, in order to prolong the module lifetime, the interconnect resistance should be as small as possible, and the module current collector should not be connected with the edge single cell.

Keywords—interconnect resistance, parallel-connected cells, current collector, LiFePO₄ battery, equivalent circuit model

I. INTRODUCTION

Electric Vehicles (EVs) receive increasing attentions in recent years, which lead to the decarbonization of the Light Duty Vehicle fleet [1, 2]. In EVs, Lithium-ion batteries (LIB) have been extensively applied in energy storage system due to their outstanding characteristics of small size, high energy density and long cycle life [3, 4]. In application, the battery module always consists of several relatively small battery cells in parallel to satisfy the required capacity and power in EVs, like Tesla Model S BMW E-Mini and Jaguar I-pace released in 2018. However, the module with parallel-connected cells is very sensitive to cell-to-cell parameter variations, a position of module current collector and interconnect resistances between parallel-connected cells, which all lead to pronounced current and state of charge (SOC) inhomogeneities [5, 6]. This not only affects the capacity of

the module, but also causes early degradation of battery and potential safety issues [7].

In most of relevant literatures, the model simulation and experimental methods were adopted to examine the parallel-connected cells with different cell parameters (such as resistance and capacity) [8-13]. Therefore, there were the abundant phenomena of inhomogeneous current and SOC distributions within the parallel-connected cells. However, previous studies seldom focused on the influence of the interconnect resistances and the position of current collector on a battery module performance. Offer al. [14] concluded that single high inter-cell contact resistance caused currents to flow unevenly within the module, and led to cells being unequally worked by a simulated model. Then Wang al. [15] simulated the effect of inter-cell connecting plate resistance on the battery module performance. Simulation results indicated that the plate resistance caused unevenly current flow. Most recently, Grün al. [16] varied the cell internal resistance, the current collector resistance and the topology of the circuitry to determine the influence of each of these parameters on the current distribution by the simulation. In summary, the simulation is an important and effective approach to study the performance of a module with parallel-connected cells.

Following the latest perspective, this paper firstly develops an equivalent circuit simulation model. Then based on the model, a module of five cells connected in parallel is established, including interconnect resistances. Moreover, the influences of interconnect resistances and different positions of module current collector in parallel-connected cells is tested and discussed by the simulation. Finally, a conclusion is presented.

II. MODEL DEVELOPMENT

A. Battery cell model

The equivalent circuit model (ECM) is widely used due to its relative simplicity, ease of parameterization and real-time feasibility [17, 18]. In this paper, the developed single cell ECM consists of several elements, as shown in Fig. 1: the open circuit voltage (OCV) U_{oc} , ohmic internal resistance R_o and two resistor-capacitor (RC) pairs, each of which is a resistor and capacitor in parallel. This is the best tradeoff between accuracy and complexity [17].

This work was supported by the National Natural Science Foundation of China (No. 61527809, 61633015, 51774193, U1764258, U1864205). Corresponding author: Linjing Xiao.

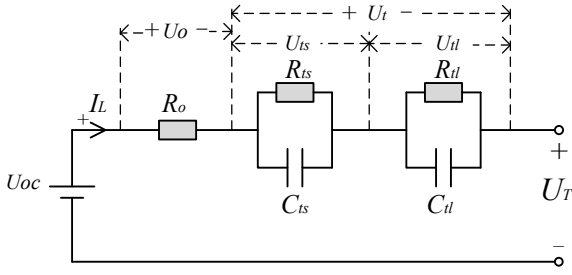


Fig. 1. Equivalent Circuit Model

The equation group Eq. (3) is obtained from Fig. 1 by using Kirchhoff's laws, where I_L is the given current, U_T is the terminal voltage and the voltage of both of the RC pairs is U_{ts} and U_{tl} respectively. The critical parameters, U_{oc} , R_o , R_{ts} and C_{tl} , are related to SOC and current in a constant-temperature application (ignoring temperature effects) [18]. Therefore, tables can quantitatively describe the relationship of SOC and current on these parameters, which need to be pre-established and pre-calibrated by experiments.

$$\begin{cases} U_T = U_{ts} + U_{tl} + I_L R_o \\ C_{ts} \frac{d}{dt} U_{ts} + \frac{1}{R_{ts}} U_{ts} = I_L \\ C_{tl} \frac{d}{dt} U_{tl} + \frac{1}{R_{tl}} U_{tl} = I_L \end{cases} \quad (1)$$

B. Identification and validation of model parameters

To establish the above mentioned tables, pulse power tests are carried out with 18650-format LiFePO₄ battery cells on a test bench. In a pulse test, there are 4 pairs of 60 second charging and discharging pulses at increasing magnitudes and scaled relative to the maximum current rate of the cell (0.2 C, 0.5 C, 1 C, 2 C), followed by a 30 min rest. The pulse test is repeated at different SOC's to capture the parameters variation across the SOC range.

Fig. 2 shows a magnified view of one discharge pulse. The transient response is characterized by two RC pairs in Fig. 2, which are responsible for short- and long-time constants of the step response, shown by the four circles in Fig. 2. By analyzing the testing data, it is found that the response of a pulse process is obviously different with a resting process, shown by the four circles in Fig. 2. And the time constant of the resting process is greater than that of the pulse process.

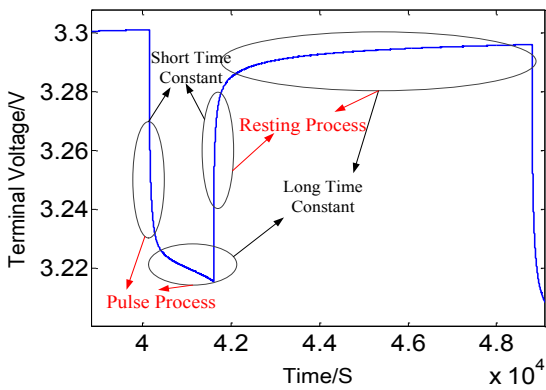


Fig. 2. The transient voltage characteristics of lithium battery

To fit the measurement data, the parameters of the ECM

are adjusted with the pattern search optimization algorithm in the program Matlab, such as a Recursive Least Squares algorithm [17]. Then the identified model parameters at different SOC's and processes are shown in Fig. 3.

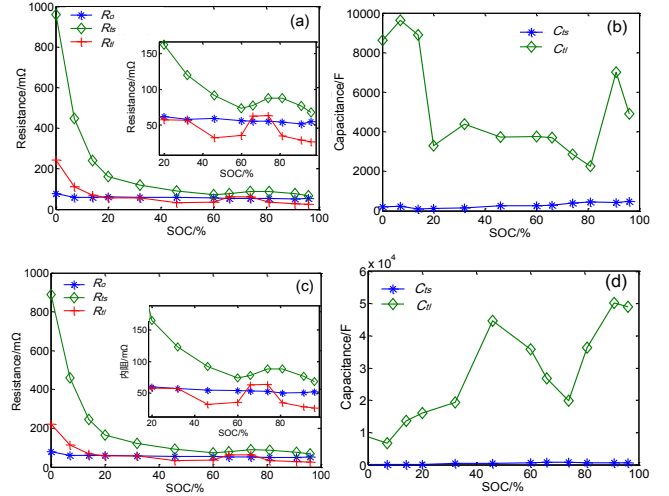


Fig. 3. Parameter identification results at different SOC: (a-b) the resistances and capacitances in the pulse process; (c-d) the resistances and capacitances in the resting process.

The nonlinear relation between the OCV and SOC is very important to be included in the model. A voltage-controlled voltage source U_{oc} is used to represent the relation, which is defined by a table that depends on the SOC in this paper. The OCV is normally measured as the steady-state terminal voltage at different SOC's. However, this measurement can take days for all SOC's. A pseudo OCV-SOC curve is obtained by discharging and charging each cell at C/25, which can save time. In this paper, a pseudo and resting OCV-SOC curve are combined to realize a precision OCV-SOC table. Fig. 4 gives the intuitive idea that it can be divided into several linear regions. Firstly, the derivative of the pseudo OCV-SOC versus should be obtained. Then the first and the second derivative of the pseudo OCV-SOC versus are used to find out the proper finite linear segments for the VOC-SOC table. At last, the OCV-SOC versus is obtained by each 2h rest at the segment points of SOC.

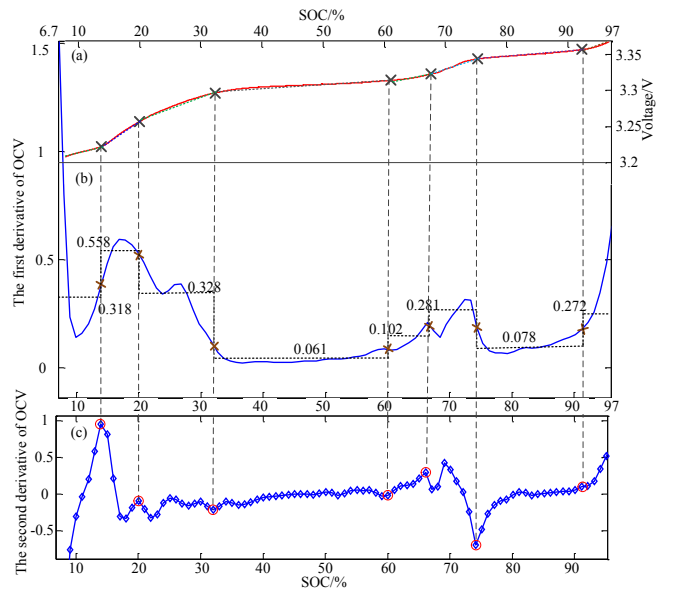


Fig. 4. OCV piecewise linear curve

C. Model validation

According to the above tables and data, an ECM of a single cell is built with the Matlab. Multiple discharge pulses test profile is employed to exercise the 18650-format LiFePO4 cell (capacity is 1.5Ah) for verifying the accuracy of the model. Fig. 5 shows the comparison of cell current, SOC, voltage and the differences between the simulation and the experiment. The simulation results agree well with the experimental data, and the maximum difference is within 1%.

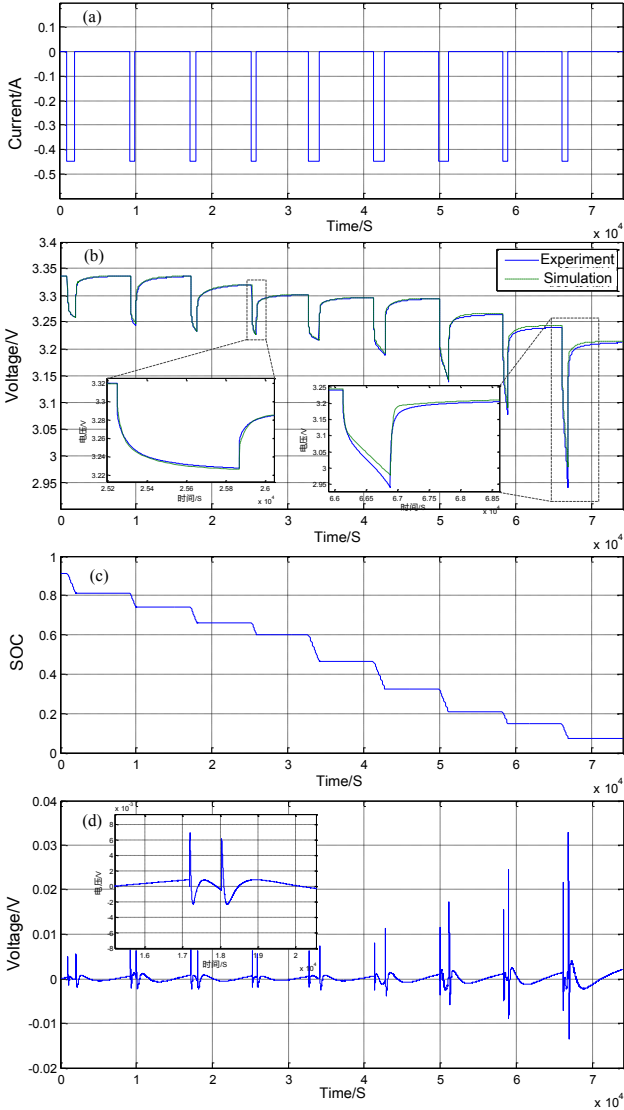


Fig. 5. Pulse discharge curves of battery simulation model

III. EFFECT OF INTERCONNECT RESISTANCES AND DIFFERENT POSITIONS OF MODULE CURRENT COLLECTOR IN PARALLEL-CONNECTED CELLS

Using the example of five cells connected in parallel as shown in Fig. 6 (a), the connecting plate is made of Nickel-plated steel due to its corrosion resistance, high mechanical stability, and good weld ability. The area of connecting plate between two adjacent cells is $20 \times 7 \text{ mm}^2$, with the thickness of 0.2mm. Then its resistance is about $1.2\text{m}\Omega$ ($R_{\text{inter}} = 1.2\text{m}\Omega$) by calculation.

A. Different positions of module current collector

In Fig. 6 (b), the solid (P1) and dotted (P2) lines show the module current collector are connected with the 5th cell and

the 3th cell, respectively. In Fig. 6 (c), the solid (P3) lines show that the positive terminal and negative terminal of module current collector are connected with the first cell positive terminal and the 5th battery cell negative terminal, respectively. Similarly, the dotted (P4) lines show that the terminals of module current collector are connected with the second and 4th cell, respectively.

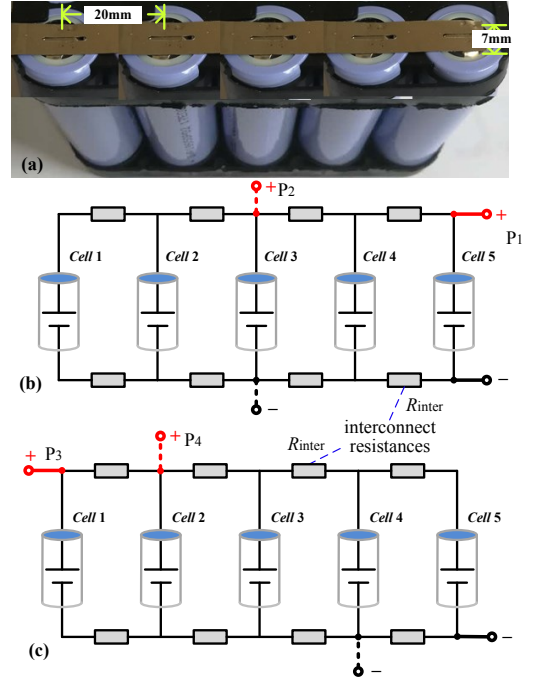


Fig. 6. (a) Five cells connected in parallel; (b-c) the different positions of module current collector.

B. Simulation

The ECM (in section 2) is assembled with the integrated cell model by the above interconnect resistances. The cells are labeled from cell1 (first) to cell5 (5th), from the left in the battery module as shown in Fig. 6. The constant current (CC) discharge is used with 1C. Four different positions (P1, P2, P3 and P4) of module current collector with $R_{\text{inter}} = 1.2\text{m}\Omega$ are tested by the simulation, as shown in Fig. 7.

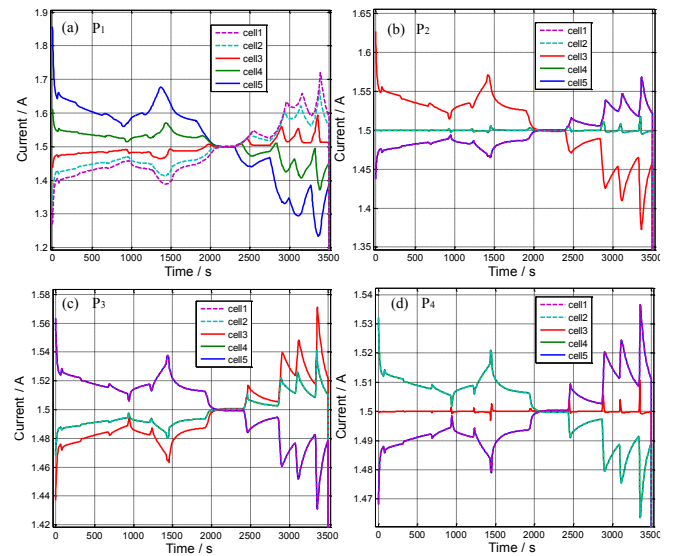


Fig. 7. Currents with different positions (P1, P2, P3 and P4) of module current collector

C. Discussion

According to Fig. 7, remarkable different currents are observed within the parallel-connected cells. The cell directly connected to the module current collector appears the highest current. The farther cell is away from the module current collector, the lower current is. Therefore, the differences among the cell currents are the lowest in P4.

In order to analyze the reasons, the current through the i th interconnect resistance I_{ci} can be calculated by Eq. 2, depending on the topology, as shown in Fig. 8 (in P1).

$$I_{ci} = \sum_{j=1}^i I_j, \quad i \in \{1, \dots, \dots, \dots\}, \quad (2)$$

where I_j is the current through the j th cell with $\sum_j I_j = 5C$. However, in P2 of Fig. 8, I_{ci} is calculated by Eq. 3. Obviously, the highest differences of current in Eq. 2 is higher than Eq. 3, which is consistent with the Fig. 7 (a) and Fig. 7 (b). There is similar situation in P3 and P4 of Fig. 7.

$$\begin{cases} I_{c1} = I_1, & I_{c4} = I_5 \\ I_{c2} = I_1 + I_2, & I_{c3} = I_4 + I_5 \end{cases} \quad (3)$$

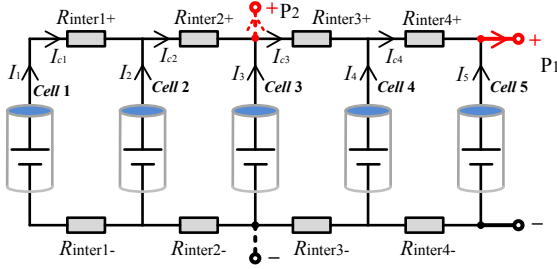


Fig. 8. the representative module for calculation currents.

The inhomogeneous currents can cause different degradation levels of the parallel-connected cells. However, in application, the module of parallel-connected cells is always treated as a unit. Therefore, in order to reduce the inhomogeneous currents, not only the interconnect resistance should be as small as possible, but also the module current collector should not be connected with the edge single cell.

IV. CONCLUSION

The CC discharge tests show that the impact of the interconnect resistance and the position of the module current collector on the performance of parallel-connected cells cannot be neglected. Thus their influences on the module performance is discussed by the simulation.

First of all, an EMC is developed with Matlab platform. The parameters of the EMC is identified, which is described by tables. This proposed model is validated by multiple discharge pulses test. The simulation results agree well with the experimental data.

Moreover, based on the model, the effect of interconnect resistances and different positions of module current collector in parallel-connected cells is discussed by simulating. Results indicate that the cell directly connected to the module current collector appears the higher current. And the farther the cell is away from the module current collector, the lower current is.

Finally, in order to reduce the inhomogeneous currents, the interconnect resistance should be as small as possible, and the module current collector should not be connected with the edge single cell.

ACKNOWLEDGMENT

The authors thank the National Natural Science Foundation of China. Furthermore, the authors thank Dr. Guanguan Zhang for suggestions and modification opinions.

REFERENCES

- [1] B. Huang, Z. Pan, X. Su, and L. An, "Recycling of lithium-ion batteries: Recent advances and perspectives," *Journal of Power Sources*, vol. 399, pp. 274-286, 2018.
- [2] A. Mahmoudzadeh Andwari, A. Pesiridis, S. Rajoo, R. Martinez-Botas, and V. Esfahanian, "A review of battery electric vehicle technology and readiness levels," *Renewable and Sustainable Energy Reviews*, vol. 78, pp. 414-430, 2017.
- [3] L. Chang, C. Zhang, T. Wang, Z. Yu, N. Cui, B. Duan and C. Wang, "Correlations of cell-to-cell parameter variations on current and state-of-charge distributions within parallel-connected lithium-ion cells," *Journal of Power Sources*, vol. 437, 226869, 2019.
- [4] N. Nitta, F. Wu, J. T. Lee, and G. Yushin, "Li-ion battery materials: present and future," *Materials Today*, vol. 18, no. 5, pp. 252-264, 2015.
- [5] S. Rothgang, T. Baumhöfer, H. van Hoek, T. Lange, R. W. De Doncker, and D. U. Sauer, "Modular battery design for reliable, flexible and multi-technology energy storage systems," *Applied Energy*, vol. 137, pp. 931-937, 2015.
- [6] B. Wu, V. Yufit, M. Marinescu, G. J. Offer, R. F. Martinez-Botas, and N. P. Brandon, "Coupled thermal-electrochemical modelling of uneven heat generation in lithium-ion battery packs," *Journal of Power Sources*, vol. 243, pp. 544-554, 2013.
- [7] Y. Kang, B. Duan, Z. Zhou, Y. Shang, and C. Zhang, "A multi-fault diagnostic method based on an interleaved voltage measurement topology for series connected battery packs," *Journal of Power Sources*, vol. 417, pp. 132-144, 2019.
- [8] R. Gogoana, M. B. Pinson, M. Z. Bazant, and S. E. Sarma, "Internal resistance matching for parallel-connected lithium-ion cells and impacts on battery pack cycle life," *Journal of Power Sources*, vol. 252, pp. 8-13, 2014.
- [9] M. Wu, C. Lin, Y. Wang, C. Wan, and C. R. Yang, "Numerical simulation for the discharge behaviors of batteries in series and/or parallel-connected battery pack," *Electrochimica Acta*, vol. 52, no. 3, pp. 1349-1357, 2006.
- [10] J. Zhang, C. Song, H. Sharif, and M. Alahmad, "Modeling discharge behavior of multicell battery," *IEEE Trans. Energy Convers.*, vol. 25, pp. 1133-1141, 2010.
- [11] S. Miyatake, Y. Susuki, T. Hikihara, S. Itoh, and K. Tanaka, "Discharge characteristics of multicell lithium-ion battery with nonuniform cells," *Journal of Power Sources*, vol. 241, pp. 736-743, 2013.
- [12] T. Bruen, and J. Marco, "Modelling and experimental evaluation of parallel connected lithium ion cells for an electric vehicle battery system," *Journal of Power Sources*, vol. 310, pp. 91-101, 2016.
- [13] M. J. Brand, M. H. Hofmann, M. Steinhardt, S. F. Schuster, and A. Jossen, "Current distribution within parallel-connected battery cells," *Journal of Power Sources*, vol. 334, pp. 202-212, 2016.
- [14] G. J. Offer, V. Yufit, D. A. Howey, B. Wu, and N. P. Brandon, "Module design and fault diagnosis in electric vehicle batteries," *Journal of Power Sources*, vol. 206, pp. 383-392, 2012.
- [15] L. Wang, Y. Cheng, and X. Zhao, "Influence of connecting plate resistance upon LiFePO4 battery performance," *Applied Energy*, vol. 147, pp. 353-360, 2015.
- [16] T. Grün, K. Stella, and O. Wollersheim, "Influence of circuit design on load distribution and performance of parallel-connected Lithium ion cells for photovoltaic home storage systems," *Journal of Energy Storage*, vol. 17, pp. 367-382, 2018.
- [17] X. Hu, S. Li, and H. Peng, "A comparative study of equivalent circuit models for Li-ion batteries," *Journal of Power Sources*, vol. 198, pp. 359-367, 2012.
- [18] C. Min, and A. R. o.-M. Gabriel, "Accurate Electrical Battery Model Capable of Battery Model Capable of Predicting Runtime and I-V Performance," *IEEE Transactions on Energy Conversion*, vol. 21, no. 2, pp. 504-511, 2006.